

Document downloaded from:

<http://hdl.handle.net/10251/95459>

This paper must be cited as:

García-Oliver, JM.; Margot, X.; Chávez Cobo, MDJ.; Karlsson, A. (2011). A combined 1D3D CFD approach for reducing mesh dependency in Diesel spray calculations. *Mathematical and Computer Modelling*. 54(7):1732-1737. doi:10.1016/j.mcm.2011.01.041



The final publication is available at

<http://doi.org/10.1016/j.mcm.2011.01.041>

Copyright PERGAMON-ELSEVIER SCIENCE LTD

Additional Information

# A combined 1D3D CFD approach for reducing mesh dependency in Diesel spray calculations

J.M. García-Oliver<sup>a,1</sup>, X.Margot<sup>a</sup>, M. Chávez<sup>a</sup>, A. Karlsson<sup>b</sup>

<sup>a</sup>*CMT - Motores Térmicos, Universidad Politécnica de Valencia, Edificio 6D, 46022, Valencia, Spain.*

<sup>b</sup>*Volvo Technology Corp., Dept. 6100, Sven Hultins Gata 9 A, Chalmers Science Park, 41288, Göteborg, Sweden.*

---

## Abstract

A 1D3D-CFD coupled spray model is proposed in this work for the simulation of Diesel sprays under non-evaporative conditions and constant injection velocity in time. The basic idea of the model is to reduce the poor estimations of the gas velocity and droplets/gas relative velocity obtained with the standard 3D-CFD Eulerian-Lagrangian spray model, when coarse meshes are used. The coupling has been achieved in the calculation of the momentum source interaction term. General considerations, descriptions and implementation of the model in a commercial CFD code are outlined. Diesel spray simulations performed using the proposed approach have been compared with those obtained with the standard 3D-CFD, 1D models and experimental data. Encouraging results were found in terms of spray evolution when changing meshes and ambient conditions.

*Keywords:* CFD, Diesel spray, 1D model

---

## 1. Introduction

The 3D-CFD Eulerian-Lagrangian approach proposed by [1, 2] was originally developed for simulating highly dispersed sprays. Nevertheless, it is commonly used for the simulation of Diesel sprays. The model solves the interaction of two phases: the continuous phase (in-cylinder gas) and the disperse one (liquid droplets). The conservation equations of mass, momentum and energy are formulated for each dispersed element in the Lagrangian form and in Eulerian form for the gas phase. The gas equations are suitably modified with source interaction terms and the void fraction in order to consider the presence of the droplets.

The void fraction is calculated in each cell and it is the ratio between the total liquid volume in a cell and the volume of such cell. In order to keep the model hypothesis of dispersed sprays, this value is very small compared to unity in many CFD codes [3, 4], restricting the use of meshes with very small

---

<sup>1</sup>Corresponding author Tel.: +34 96 387 76 50; fax: +34 96 387 76 59. E-mail address: jgarciao@mot.upv.es

cell size. However, performing spray simulations with coarse meshes leads to poor estimations of the numerical spray evolution [5, 6].

As nowadays fuel injection pressures are very high, nozzle hole diameters are very small and air density inside the combustion chamber is also high, the complete atomization regime is reached very near the nozzle exit. Therefore, the assumptions of mixing controlled hypotheses for Diesel sprays are valid, and they can be analysed from a point of view of gas jet theory [7]. The One-dimensional (1D) Eulerian model based on this analogy simplifies the calculation of complicated two-phase flows by defining an equivalent one-phase flow instead with a mesh-independent formulation.

In this work the equations and strategies for obtaining a coupled 1D3D-CFD spray model are presented, which aims to improve the calculation predictions and reduce mesh dependency of the 3D-CFD standard model. The coupling is achieved in the momentum source interaction term calculation, where CFD axial gas velocity is replaced by the gas jet velocity. Even though this idea has been proposed before [8, 9], the contribution of this research is based on the methodology for the implementation in the commercial *STAR-CD* CFD code, and it is also a continuation of the original 1D formulation developed by [7].

## 2. 3D-CFD Eulerian-Lagrangian spray model

The conservation equations for the gas/droplets phases are solved in the 3D-CFD Eulerian-Lagrangian framework in *STAR-CD* code. The Eulerian gas conservation equations are suitably modified to consider the presence of the droplets. In a Lagrangian formulation, droplets are statistically grouped in computational “parcels” having the same properties, which are tracked in position and time during the calculation period. The movement of the droplet during the computational time step  $\delta t$  is determined from Newton’s law. In this work, only the drag force  $\vec{F}_D$  will be considered, which is caused by the relative velocity of the droplet to the surrounding gas phase and given by:

$$m_d \frac{\delta}{\delta t} \vec{u}_d = \vec{F}_D = \frac{1}{2} \rho_a C_D A_d |\vec{u} + \vec{u}' - \vec{u}_d| (\vec{u} + \vec{u}' - \vec{u}_d), \quad (1)$$

where  $m_d$  is the droplet mass,  $\rho_a$  is the air density,  $C_D$  is the drag coefficient for ideally spherical droplets,  $A_d$  is the cross section droplet area,  $\vec{u}_d$ ,  $\vec{u}$ ,  $\vec{u}'$  are droplet, mean gas and turbulent fluctuation velocities, respectively. The magnitude of the relative velocity is  $U_r = |\vec{u} + \vec{u}' - \vec{u}_d|$ .

Spray sub-models are used in the 1D3D model in order to simulate different spray phenomena. Primary atomization has been modeled by the Huh-Gosman (HG) model [10]. Secondary atomization or break-up has been modeled with the Hsiang-Faeth approach (HF) [11, 12]. The calculation of the spray droplet dispersion due to a turbulent flow field interaction has been carried out with the numerical method proposed by O’Rourke [13], which has been implemented in the spray model replacing the default model available in *STAR-CD* [3].

## 3. 1D-Eulerian spray model

The 1D-Eulerian spray model allows to represent the 3D two-phase transient spray problem in a 2D single-phase steady spray problem. Figure 1-a depicts a transient spray injected with constant nozzle exit velocity. Two different regions

can be observed in the spray: the steady and the transient ones. In Figure 1-b the same spray has been schematically represented using the turbulent gas jet analogy, which divides the steady region in two sub-zones: the intact core and the fully-developed turbulent flow. In the intact sub-zone, fuel on the spray axis has not been affected by the entrained air (on-axis velocity equal to injection velocity). In the main or fully-developed turbulent sub-zone fuel in the whole section of the spray has been perturbed, and radial profiles of axial velocity are self-similar. The transient region of the spray, located at the spray tip, is not studied by this methodology.

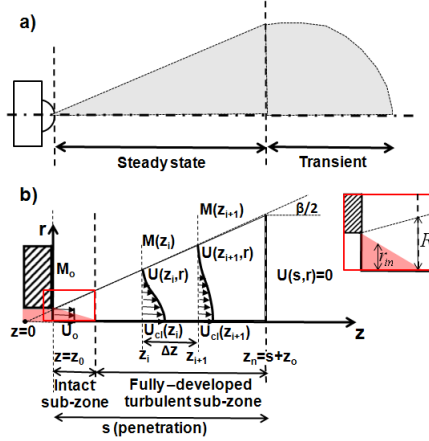


**Figure 1:** (a) Example of a spray and its regions, (b) schematic of a spray modelled as a turbulent gas jet.

In Figure 1-b, the coordinate system  $(z, r)$  is located at the origin of the jet,  $z$ -coordinate coincides with the spray axis and  $r$ -coordinate is the radial position. For constant injection velocity the momentum flux  $M(z)$  is conservative in any section perpendicular to the spray axis in the steady sub-zone, i.e.  $M_0$  is equal to  $M(z)$  (subscripts 0 and  $z$  denote the momentum flux through the orifice outlet and a spray cross-section at a distance  $z$ , respectively). The 1D model uses radial profiles to transform a 2D problem  $(z, r)$  into 1D problem and solves the axial velocity field  $U(z, r)$  from the momentum flux. In the intact sub-zone, depending on the axial and radial position of the droplet, a Semi-Gaussian radial profiles for the gas velocity has been used:

$$U(z, r) = \begin{cases} U_0, & r \leq r_{in} \\ U_0 \exp \left[ -4.6052 \left( \frac{r-r_{in}}{R-r_{in}} \right)^2 \right], & r > r_{in}, \end{cases} \quad (2)$$

where  $r_{in}$  is the inner radius and  $R$  is the external radius defining the intact core region and the spray limit, respectively.

Under fully-developed turbulent flow assumptions, the ratio of any conserved variable divided by the centerline value does not depend on the axial coordinate,

thus the velocity radial profile can be Gaussian type and expressed as [7]:

$$U(z, r) = U_{cl}(z) \exp \left[ -\frac{4.6052}{\tan^2(\beta/2)} \left( \frac{r}{z} \right)^2 \right], \quad (3)$$

where  $r$  is any radial position,  $U_{cl}(z)$  is the gas velocity on the spray axis (centerline), which is inversely proportional to the axial distance  $z$ , and  $\beta$  is a measure of the spray dispersion.

#### 4. Coupling methodology

Gas jet axial velocity  $U(z, r)$  from the 1D model replaces the CFD gas axial velocity  $U_z$  in the calculation of the relative velocity  $U_r$  and in the near nozzle zone. The 1D3D coupling is performed only from the nozzle exit until a certain distance, which is defined as  $mIL$ , where  $IL$  is the gas jet intact sub-zone length (i.e. distance in which  $U_{cl}$  is equal to  $U_0$ ) and  $m = 5$ . The methodology of the 1D3D coupling is explained through figures Fig. 2-a and 2-b, where the CFD spray evolution, a representation of the radial gas velocity profiles and the gas axis velocity imposed are shown for two different calculation times  $t_i$  and  $t_j$ .

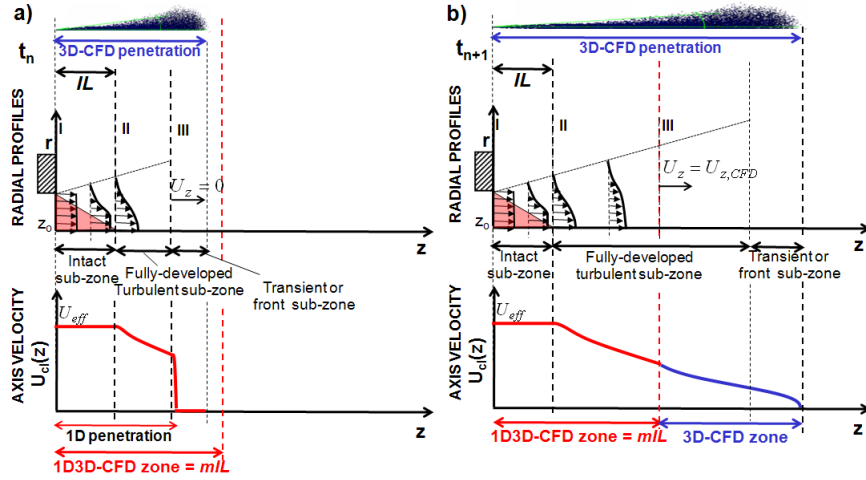


**Figure 2:** Scheme of the corrected CFD spray evolution for two different calculation times a)  $t_i$  and b)  $t_j$ .

In a spray with smaller penetration than the 1D3D-CFD zone limit  $mIL$  (Fig. 2-a),  $U_z$  is calculated using Eq.(2) for the intact-sub-zone region, by means of Eq.(3) for the turbulent-developed sub-zone and is zero for the region between the 1D spray penetration and the 3D-CFD spray penetration.

In a spray with larger penetration than the corrected zone  $mIL$  (Fig. 2-b),  $U_z$  is calculated using Eq.(2) for the intact-sub-zone region, by means of Eq.(3) for the turbulent-developed sub-zone and calculated by the default CFD code after the corrected zone.

## 5. Simulated cases

The general set-up used for the 3D-CFD and 1D-Eulerian spray calculations are described in Table 1:

**Table 1:** Spray models set-up.

	3D-CFD Eulerian-Lagrangian		1D-Eulerian
<b>Boundary conditions</b>	Inlet	- Flow injection and nozzle geometric parameters. - Total number of parcels injected of $5e^{+06}$ /s. - Droplets introduction in cell vertex at the local cylindrical coordinate system. - Air/fuel thermodynamic properties.	- Flow injection parameters (mass flow and momentum flux). - Effective orifice diameter.
	Walls	No slip conditions and droplets impact.	- Air/fuel thermodynamic properties.
<b>Numerical aspects</b>	- Transient PISO (coupled procedure) [3]. - Computational time step of $1e^{-6}$ s.		Solution procedure description in [7].
<b>Turbulence</b>	k- $\epsilon$ High Reynolds Numbers model ( $C_{\epsilon 1}=1.60$ [14]).		X

Four different 3D meshes have been used in the calculations. All meshes present a cylindrical geometry, 100 mm in diameter and 152 mm in length. The cell size along the spray axis is kept constant. The specifications of the meshes are presented in Table 2. Non-vaporising spray experimental data from the work published by Naber and Siebers [15] have been used for the model validation. Specifically, sprays injected with the single-orifice nozzle of  $D_n=257 \mu\text{m}$  in nominal diameter and for two air densities  $\rho_a = 14.8 \text{ kg/m}^3$  (A cases) and  $\rho_a = 30.0 \text{ kg/m}^3$  (B cases). The whole matrix has been simulated with the standard 3D-CFD, the 1D3D-CFD and the 1D spray models, the latter one used as reference in the next section.

**Table 2:** Specification of the 3D meshes and calculation matrix.

Meshes	Cells number	Cell size near the injection point (mm)	Cases	$\rho_a$ (kg/m <sup>3</sup> )
M1	144500	0.5x0.5x1.0	1A/1B	14.8/30.0
M2	75480	0.75x0.75x1.5	2A/2B	14.8/30.0
M3	36328	1.0x1.0x2.0	3A/3B	14.8/30.0
M4	29184	2.0x2.0x2.0	4A/4B	14.8/30.0

## 6. Results and discussion

### 6.1. Spray penetration

In Figures 3-a and 3-b Diesel spray tip penetration as a function of time is shown for A and B cases of Table 2, respectively. Solid and dashed lines correspond to the simulated spray penetration and symbols represent the experiments. In both figures, the 3D-CFD standard spray simulations (left) are compared with the 1D3D-CFD spray simulations (right).

In the zone closest to the nozzle, penetration results from the 1D3D model overlap independently of the mesh size. This is not the case in the 3D standard model, where a high sensitivity to mesh size is observed. This mesh independency extends until the spray reaches the end of the corrected zone ( $5IL=30.5$  mm for cases with  $\rho_a = 14.8 \text{ kg/m}^3$  and  $5IL=18.1$  mm for cases with  $\rho_a = 30.0$

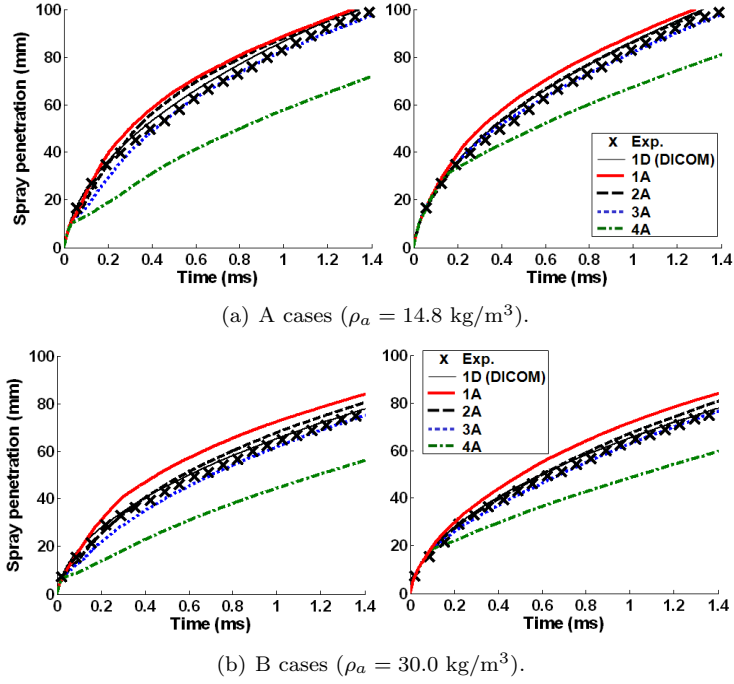


**Figure 3:** Spray tip penetrations. Simulations with the 3D-CFD standard spray model (left) and with the 1D3D-CFD spray model (right).

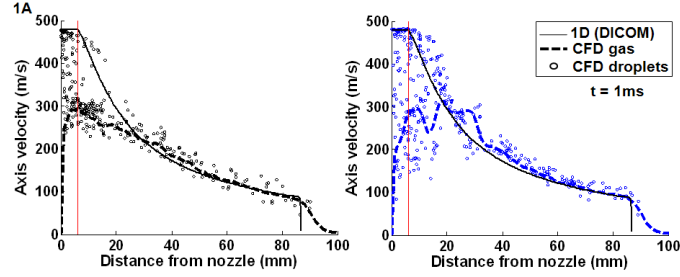
$\text{kg/m}^3$ ). In the non-corrected zone of the spray, 1D3D penetration curves tend to diverge in the same way as 3D standard penetrations. However, for both air densities, differences between M1 and M4 penetrations calculated with the 1D3D model have been reduced considerably compared with the 3D standard model. Thus, it can be concluded that using the 1D3D spray model, less mesh sensitive results can be obtained. Moreover, spray penetration obtained with the 1D3D model shows an evolution closer to experimental results.

### 6.2. On-axis spray velocity

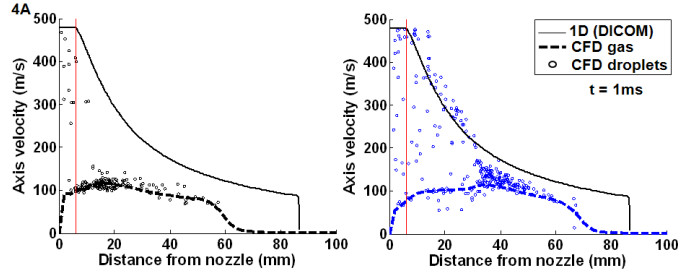
Figures 4-a and 4-b depict on-axis spray velocities for the liquid (droplets) and gas phase as a function of the axial distance ( $t=1\text{ms}$ ) for low air density cases (1A and 4A, i.e. finest vs. coarsest meshes) simulated with the 3D standard model (left) and with the 1D3D coupled model (right). Symbols represent droplet velocity and dashed lines correspond to gas velocity. In this case, there are no available experimental data, so the reference single-phase on-axis velocity from the 1D model is also plotted. The vertical line defines the end of the intact sub-zone length ( $IL=6.09 \text{ mm}$ ). The typical drop of the axis velocity with axial distance can be observed with the three models, which results from the increase of air entrainment along the spray evolution.

Up to an axial distance of  $5IL$ , liquid phase velocities calculated with the 1D3D model are higher compared to liquid phase velocities from the 3D model

for all cases. This results in a slower acceleration of the gas phase for 1D3D calculations compared to 3D standard simulations. After  $5IL$ , all 3D-CFD simulations both phases have reached dynamic equilibrium. Nevertheless, droplets/gas on-axis velocities are closer to the reference 1D spray on-axis velocity when calculations are carried out with the 1D3D spray model, especially for the coarser mesh.



(a) 1A case ( $\rho_a = 14.8 \text{ kg/m}^3$ ).



(b) 4A case ( $\rho_a = 14.8 \text{ kg/m}^3$ ).

**Figure 4:** Spray on axis velocities. Simulations with the 3D-CFD standard spray model (left) and with the 1D3D-CFD spray model (right).

## 7. Conclusions

A coupled 1D3D-CFD Eulerian-Lagrangian spray model for the simulation of Diesel sprays in non-vaporising conditions and constant injection velocity profiles has been presented. A description of the main assumptions and methodology for the implementation in the commercial *STAR-CD* CFD code has been outlined. The background solver for the droplets/gas conservation equations is the two-phase 3D-CFD Eulerian-Lagrangian framework where the 1D-Eulerian spray model takes part in the correction of the droplets/gas relative velocity calculation and hence, in the calculation of the momentum source interaction term.

Diesel spray simulations with the proposed model have been carried out using four meshes with different cell sizes and two ambient conditions ( $\rho_a = 14.8 \text{ kg/m}^3$  and  $\rho_a = 30.0 \text{ kg/m}^3$ ). Results were analysed for the spray penetration and on-axis velocity profile. In general, all simulations carried out with the 1D3D spray model show enhance accuracy in terms of both variables studied.



The mesh independence in 1D3D spray penetrations has been totally achieved in the corrected-zone and improved in the non-corrected zone.

#### **Acknowledgements**

This work has been founded by Universidad Politécnica de Valencia UPV under the FPI-UPV program and the public project TRA2007-68006-C02-01, from MICINN (Spain). Special thanks are extended to Dr. S. Hoyas and Dr. J.M. Pastor and Dr. M. Balthasar for the support and motivation.

#### **References**

- [1] J.K. Dukowicz. A Particle-Fluid Numerical Model for Liquid Sprays. *J. of Computational Physics* 35, 229-253, 1980.
- [2] P.J. O'Rourke and F.V. Bracco. Modeling of Drop Interaction in Thick Sprays and a Comparison with Experiments. IME Stratified Charge Automotive Engines Conference, London, 1980.
- [3] Computational Dynamics Ltd., STAR-CD V.3.26 - Methodology, 2005.
- [4] A. Amsden, P. J. O'Rourke and T. D. Butler, KIVA-II: A Computer Program for Chemically Reactive Flows with Sprays, Technical report No. LA-11560-MS, Los Alamos National Laboratory, May, 1989.
- [5] S. Post, V. Iyer and J. Abraham. A study of the Near-Field Entrainment in Gas Jets and Sprays Under Diesel Conditions, *ASME J. of Fluid Engineering* 122, 385-395, 2000.
- [6] D. P. Schmidt and P.K. Senecal. Improving the Numerical Accuracy of Spray Simulations. SAE Paper 2002-01-1113, 2002.
- [7] José V. Pastor, J. Javier López, José M. García and José M. Pastor. A 1D model for the description of mixing-controlled inert Diesel sprays, *Fuel* 87, 2871-2885, 2008.
- [8] X. Yang, Y. Takamoto and A. Okajima. Improvement of Three-Dimensional Diesel Spray Modeling in Near Region with Coarse Mesh, SAE Paper 2000-01-0274, 2000.
- [9] Y. Wang, Hai-Wen Ge and R.D. Reitz. Validation of Mesh and Timestep-Independent Spray Models for Multi-Dimensional Engine CFD Simulation. SAE Paper 2010-01-0626, 2010.
- [10] K.Y. Huh and A.D. Gosman. A Phenomenological Model of Diesel Spray Atomization, Proc. Int. Conf. on Multiphase Flow, Japan, 24-27, 1991.
- [11] L.P Hsiang and G.M. Faeth. Near-limit Drop Deformation and Secondary Breakup, *Int. J. Multiphase Flow* 18(5), 635-652, 1992.
- [12] X. Margot, R. Payri, A. Gil, M.Chávez and A. Pinzello. Combined CFD-Phenomenological Approach to the Analysis of Diesel Sprays Under Non-evaporative conditions. SAE Paper 2008-01-0962.
- [13] P.J. O'Rourke. Statistical Properties and Numerical Implementation of a Model for Droplet Dispersion in a Turbulent Gas. *J. of Computational Physics* 83, 345-360, 1989.
- [14] B.B. Dally, D.F. Fletcher. and A.R. Masri. Flow and Mixing Fields of Turbulent Bluff-Body Jets and Flames, *Combust. Theory Modelling*, 2, 193-219, 1998.
- [15] J.D. Naber and D.L. Siebers. Effects of Gas density and Vaporization on Penetration and Dispersion of Diesel Sprays. SAE Paper 960034, 1996.